COMBINED EFFECTS OF TANNATE AND AGEING ON STRUCTURAL AND SURFACE PROPERTIES OF ALUMINUM PRECIPITATES

G. Yu[1,2], U. K Saha[1], L. M. Kozak[1] and P. M. Huang[1,*]

[1] Department of Soil Science, University of Saskatchewan, 51 Campus Drive, Saskatoon, SK, S7N 5A8, Canada
[2] Institute of Soil Science, Chinese Academy of Sciences, Nanjing, China

Abstract—The influence of organics on the crystallization of Al precipitates has been well documented. However, the effects of organics and ageing on the transformation and structural configuration of Al precipitates in relation to their surface and charge properties are not fully understood. This study investigated the structural, microporous and surface properties of Al precipitates formed under the influence of tannate and ageing. The Al precipitates were synthesized at an initial Al concentration of 7×10^{-3} M, an OH/Al molar ratio (MR) of 3.0, and initial tannate/Al MRs of 0, 0.001, 0.01 and 0.1, and aged for 1, 10 and 40 days. As indicated by a decrease in gibbsite and bayerite and an increase in the oxalate-extractable Al contents, the non-crystalline precipitates increased with the increase of the initial tannate/Al MR. This observation is in accord with the X-ray diffraction and Fourier transform infrared (FTIR) data. The impact of tannic acid on the nature of the Al precipitates is also reflected in the increase of the contents of the pyrophosphate-extractable Al, which is indicative of organically bound Al. This observation is in agreement with the increase in the intensity of characteristic FTIR absorption bands of tannate and the organic C and adsorbed water contents. The decrease in the crystallinity of Al precipitates with increase in the tannate/Al MR resulted in the development of microporosity, increase in BET specific surface area and decrease of the average pore diameter and point of zero salt effect (PZSE). The FTIR absorption bands characteristic of tannate of the Al precipitates became weaker with ageing, in accord with the ageing-induced decrease in the contents of organic C and pyrophosphate-extractable Al. Ageing drastically decreased the BET specific surface area of the Al precipitates formed in the absence of tannate but this effect was less conspicuous for the products formed at the tannate/Al molar ratio of 0.1. The ageing-induced change in the PZSE of the Al precipitates formed both in the absence and presence of tannate was not significant. The results accomplished in this study are of fundamental significance to our understanding of the combined effects of organics and ageing on structural configuration of hydrolytic precipitates of Al in relation to their microporosity, surface and charge properties in the environment.

Key Words—Ageing, Al Precipitates, Microporosity, Structural Perturbation, Surface Properties, Tannic Acid.

INTRODUCTION

Aluminum, as the third most abundant element in the Earth's crust, is ubiquitous in mineral soils. Upon the release of Al from soil minerals to slightly acidic soil solutions and natural waters through chemical weathering, it undergoes hydrolysis (Huang *et al.*, 2002). This results in the formation of a series of Al hydrolytic aqueous species and precipitates (*e.g.* gibbsite) that vary in structural order, ranging from the very crystalline to the poorly crystalline and non-crystalline. Precipitates of Al with different degrees of crystallinity vary in their charge characteristics and surface features, and consequently in their adsorption capacity for nutrients and environmental pollutants (Huang, 1988; Sposito, 1996; Huang *et al.*, 2002). Thus, the degree of crystallinity of Al precipitates is a key factor in influencing the transport, dynamics and fate of nutrients and pollutants in terrestrial and aquatic environments.

The crystallinity and reactivity of Al (oxy)hydroxide precipitates are influenced by many factors. The effects of some selected organic acids on the crystallinity of Al precipitates have been investigated extensively since the 1970s (Kwong and Huang, 1975, 1977, 1978, 1979a, 1979b, 1981; Kodama and Schnitzer, 1980; Violante and Violante, 1980; Violante and Huang, 1984, 1985; Singer and Huang, 1990; Colombo *et al.*, 2004). Some organic acids are ubiquitous in natural environments (Stevenson, 1994). The ability of low-molecular-mass organic acids to hinder crystallization of Al precipitates is closely related to their ability to complex with Al, which is reflected in the stability constants of their complexation with Al (Kwong and Huang, 1979b, 1981). The greater the stability constant of the Al-organic complex, the greater is the ability to disrupt the hydroxyl bridging mechanism instrumental in the hydrolysis of Al and hinder the crystallization of Al precipitation (Huang *et al.*, 2002). The net result is the formation of short-range ordered Al precipitates which have more reactive sites on their surfaces (Kwong and Huang, 1979a, 1979b). The greater the concentration of organic acids and the affinity of organic acids to Al, the more disordered the structure is (Huang, 1988; Huang *et al.*, 2002).

* E-mail address of corresponding author:
pmh936@mail.usak.ca

369

Tannic acid is a yellowish complex organic compound present in certain plants (Daintith, 1990). It may be flavanol-based or gallic acid-based. Both kinds of tannic acid are high-molecular-mass organic acid, contain carboxyl (COOH) groups like low-molecular-mass aliphatic organic acids. They also resemble high-molecular-mass humic substances such as fulvic acid, as they contain phenolic hydroxyl (OH) and ketonic (C=O) groups (Huang, 1995). X-ray diffraction (XRD) data from earlier investigations showed that tannic acid disturbs the crystallization of Al precipitates, resulting in the formation of poorly crystalline to non-crystalline Al precipitates (Kwong and Huang, 1981). It was inferred that the incorporation of tannate ligands into the internal structural network inhibited macro-crystallization of the Al precipitates (Kwong and Huang, 1981; Violante and Huang, 1989; Colombo *et al.*, 2004). However, the combined effects of organic acids and ageing on the nature of Al precipitates and their surface and charge properties have not been well documented.

Therefore, the objective of this study was to investigate systematically the effects of ageing and tannic acid concentration on the precipitation of Al (oxy)hydroxides. We employed an array of experimental techniques including XRD, FTIR and ^{13}C CPMAS NMR spectroscopies, organic C analysis, and selective dissolution analysis of the Al precipitates. Furthermore, the transformation and structural configuration of the Al precipitates, in relation to their microporosity and surface-charge properties, were investigated.

MATERIALS AND METHODS

Preparation of Al (oxy)hydroxide precipitates

A 200 mL aliquot of a 7×10^{-3} M $AlCl_3$ solution was mixed with 0, 1, 10 and 100 mL of 1.4×10^{-3} M tannic acid (ACS reagent, $C_{76}H_{52}O_{46}$, FW 1701.20, ignition residue $\leqslant 0.5\%$, Aldrich Chemical Company) solution in a 1000 mL pyrex Erlenmeyer flask to give initial tannate/Al molar ratios (MRs) of 0, 0.001, 0.01 and 0.1. Each of the resultant mixtures was then slowly titrated with a 42 mL aliquot of 0.1 M NaOH solution to reach an OH/Al MR of 3.0 under vigorous stirring with a magnetic stirrer. The rate of NaOH addition was 2.5 mL min^{-1}. After titration, the suspensions with initial tannate/Al MRs of 0 and 0.1 were aged for 1, 10 and 40 days. The suspensions with initial tannate/Al MRs of 0.001 and 0.01 were aged for 40 days. All mixing, titrating and ageing were performed at room temperature (~25°C). During ageing, the suspensions were gently agitated once a day. After the ageing periods, the suspensions were ultrafiltered through a Millipore membrane filter (0.1 μm pore size). The precipitates were repeatedly washed with distilled-deionized water until the electrical conductivity of the filtrate was <5 μS/cm. The precipitates obtained were freeze dried at −40°C and then stored in desiccators containing $CaCl_2$

at room temperature for use in subsequent investigations on their chemical, mineralogical, surface and charge properties.

XRD and FTIR analysis

20 mg of each Al precipitate was powder-mounted on a glass slide using one drop of acetone and analyzed by XRD with FeKα radiation generated at 40 kV and 160 mA using a Rigaku X-ray diffractometer (Rigaku Rotaflex Model RU-200) equipped with an incident-beam graphite monochromator. The XRD patterns were recorded from 4 to 60°2θ with 0.02°2θ steps at a scanning rate of 10°2θ min^{-1} in continuous mode. The preparation of all the powder-mounted slides was conducted in the same manner.

The FTIR spectra of samples were recorded on a Bruker Fourier transform infrared spectrophotometer (Tensor 27, Bruker company) using the KBr pellet technique. The KBr pellets were prepared by mixing gently and thoroughly 1 mg of slightly ground sample with 200 mg of oven-dried (at 105°C) KBr and then pressing the mixture into a disc. The FTIR spectra were collected at 4 cm^{-1} resolution, averaging 30 scans per spectrum. The spectra were analyzed with the OPUS V.4.2 software. Spectroscopic ellipsometry measurements were made within the 245−1000 nm range using a J.A. Woolam Inc. M2000 ellipsometer running the WVASE 32 software at an angle of incidence of 75.14°.

^{13}C CPMAS NMR analysis

Tannic acid and the Al precipitates formed at an initial tannate/Al MR of 0.1 were examined by ^{13}C CPMAS NMR analysis. High-resolution solid-state ^{13}C CPMAS NMR spectra were obtained at a temperature of 295 K on a Bruker Avance DRX spectrometer equipped with a 7 mm MAS probe, a rotor spin oscillation of 5000 Hz, a contact pulse 1000 μs, and a line broadening of 80 Hz. A pulse program (CPTOSSA) was adopted which suppresses spinning side bands. Adamantane was used as the standard, with the chemical shift at 38.5 ppm.

Determination of total Al, organic carbon and adsorbed water contents

Aluminum precipitates were digested with hydrofluoric acid in a 25 mL polypropylene centrifuge tube (Lim and Jackson, 1982) and the Al concentration of the digest was determined by atomic absorption spectrophotometry (AAS) at a wavelength of 309.3 nm using a Varian flame atomic absorption spectrophotometer (Model SpectrAA 220 Varian Australia Pty Ltd, Walnut Creek, California). The organic carbon content of Al precipitates was determined following the dry combustion method of Wang and Anderson (1998) based on the loss of mass upon ignition at 850°C using a Leco CR12 C analyzer (Leco Corp., St. Joseph, Michigan). The adsorbed water content of the freeze-dried pre-

cipitates was determined by heating samples to 110ºC and determining the mass loss (Gardner, 1986).

Selective dissolution analysis

Sodium pyrophosphate and acid ammonium oxalate were used to extract organically bound and non-crystalline Al fractions from the Al precipitates, respectively (Bertsch and Bloom, 1996; McKeague and Day, 1966). 10 mL of 0.1 M sodium pyrophosphate was added to 10 mg of freeze-dried Al precipitates. The suspensions were reciprocally shaken for 16 h and then centrifuged at 15,000x*g* for 30 min. The supernatant liquids were analyzed for Al by AAS (Bertsch and Bloom, 1996). Acid ammonium oxalate extraction was performed by suspending 10 mg of an Al precipitate in 10 mL of 0.2 M ammonium oxalate acidified to pH 3 in 50 mL centrifuge tubes. The suspensions were then shaken in the dark on a reciprocating shaker for 4 h, centrifuged at 15,000x*g* for 30 min, and then the supernatant liquid was collected for Al determination by AAS (Bertsch and Bloom, 1996).

Specific surface area and surface porosity

The specific surface area of the Al precipitates was determined by a gravimetric method based on the retention of ethylene glycol monoethyl ether (EGME) (Eltantaway and Arnold, 1973), and by the method based on a multiple point Brunauer-Emmet-Teller (BET) liquid N_2 adsorption isotherm (at -195ºC) (Gregg and Sing, 1982) obtained using an ASAP2000 Surface Area Analyzer (Micromeritics Instrument Corporation, Norcross, GA, USA). Prior to N_2 adsorption, a 200 mg sample was degassed at ambient temperature for 24 h at 10 mTorr. During N_2 adsorption the solids were thermostated in liquid N_2 (77$-$78 K). In addition, the pore specific surface area and average pore diameter of the Al precipitates were determined from the N_2 adsorption isotherms following the t-plot method (de Boer *et al.*, 1966; Gregg and Sing, 1982) and using the Kelvin equation assuming cylindrical pores (Storck *et al.*, 1998; Ravikovitch and Neimark, 2000).

Determination of point of zero salt effect (PZSE)

The point of zero salt effect (PZSE) of the Al precipitates was determined by locating the point of intersection of pH difference (ΔpH) between before and after salt addition (to suspensions with various pHs) *vs.* pH (Sakurai *et al.*, 1988). 10 mg of a sample were suspended in 20 mL of distilled-deionized water in a 50 mL centrifuge tube using a vortex mixing device. A series of ten such tubes was prepared for each sample, their pH was adjusted to 3, 4, 5, 6, 7, 8, 9, 10, 11 and 12 using 0.01 M HNO_3 or 0.01 M NaOH, and allowed to stand for 24 h with six interim readjustments of their pH. After 24 h, 1 mL of 0.01 M $NaClO_4$ salt solution was added to each tube, mixed well, and their pH was determined. The magnitude of pH change (ΔpH) after

salt addition to the suspensions was calculated and plotted (*y* axis) *vs.* their pH before salt addition (*x* axis) and regression analysis was used to relate ΔpH to pH. The point of intersection of this curve with the *x* axis was taken as the PZSE (Sakurai *et al.*, 1988).

RESULTS AND DISCUSSION

XRD patterns

In the absence of tannic acid, hydrolytic precipitates of Al formed at an initial Al concentration of 7×10^{-3} M and an OH/Al molar ratio of 3 were crystalline to X-ray diffraction after 1 day of ageing (Figure 1a); the crystalline species identified in the precipitate (Figure 1a) were bayerite [α-$Al(OH)_3$; 4.68, 2.21 and 3.18 Å] and gibbsite [γ-$Al(OH)_3$); 4.34 and 4.80Å] (Berry, 1974; Hsu, 1989). As the ageing period increased from 1 to 10 days, the peaks associated with bayerite and gibbsite became more intense (Figure 1b). As the ageing increased to 40 days, all of the peaks of the crystalline Al precipitates were generally sharpened and intensified, indicating that the crystallization of bayerite and gibbsite proceeded gradually with time.

The Al precipitates formed at an initial tannate/Al MR of 0.1 after ageing for 1, 10 and 40 days were X-ray amorphous, as indicated by the broad diffraction between ~12 and 44º2θ (Figure 2). The presence of tannic acid even at an initial tannate/Al MR of as little as 0.001 was able to influence the crystallization of Al precipitates (Figure 3b), as can be seen by the fact that the XRD peaks of bayerite and gibbsite were not as intense as those of the corresponding products formed in the absence of tannic acid (Figure 3a). As the initial tannate/Al MR was increased further to 0.1, the resultant Al precipitates became virtually non-crystalline according to XRD even after 40 days of ageing (Figure 3d). At the initial tannate/Al MR of 0.01, the Al precipitates show very weak diffraction peaks at 2.32, 3.13 and 6.37 Å (Figure 3c), indicating the presence of poorly crystalline boehmite.

The impeding effects of tannic acid on the crystallization of Al precipitates are attributed to: (1) the complexation of tannic acid with Al and attendant inhibition of hydrolysis of the positively charged edge Al atom of the hydroxyl-Al polymers; and (2) the occupancy of the coordination sites of Al by tannate and resultant distortion of the arrangement of the polymeric hexagonal unit layers (Kwong and Huang, 1981; Violante and Huang, 1989; Huang, 1995). The XRD data obtained in the present study are in good agreement with the work of Kwong and Huang (1981) who also reported the perturbation of crystallization when the Al precipitate was synthesized in the presence of tannate. Furthermore, our data (Figure 2) indicate that even 40 days of ageing did not result in any discernable changes in the XRD patterns of the Al precipitates formed at a high initial tannate/Al MR of 0.1.
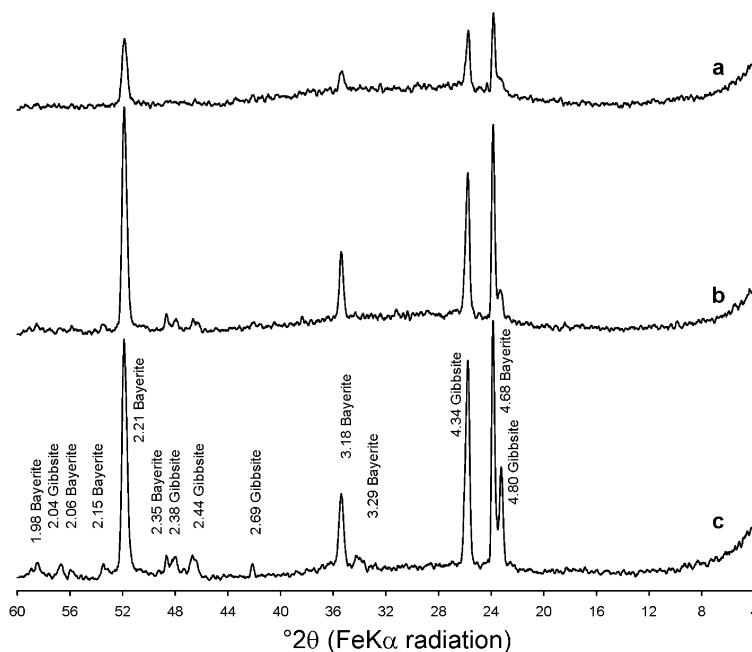
Figure 1. XRD patterns of Al precipitates formed in the absence of tannate after ageing for: (a) 1 day; (b) 10 days; and (c) 40 days. The *d* values in all patterns here are given in Å.

FTIR spectra

The FTIR spectrum (Figure 4a) shows that the Al precipitates formed in the absence of tannic acid, and after 1 day of ageing were indeed a mixture of bayerite (3656 and 769 cm^{-1}) and gibbsite (3615, 3539, 3526, 3465, 3432, 1024, 970, 559, 532 and 430 cm^{-1}) (van der Marel and Beutelspacher, 1976). The FTIR spectra characteristic of bayerite and gibbsite became sharper as the ageing period increased from 1 to 40 days (Figure 4). The results obtained from FTIR spectra (Figure 4) are consistent with those from the XRD patterns (Figure 1).

The Al precipitates formed at a tannate/Al MR of 0.1 after 1 day of ageing did not show any FTIR absorption bands characteristic of gibbsite or bayerite (compare Figures 4 and 5). However, a series of new bands (in the 1206−1700 cm^{-1} region) was evident (Figure 5a). Goh

and Huang (1986) reported characteristic strong IR absorption bands of tannate at 1725, 1620, 1545, 1445, 1330 and 1220 cm^{-1}. The corresponding bands in Figure 5 are at 1700, 1598, 1501, 1442, 1363, 1305 and 1206 cm^{-1}; the observed shift in the IR absorption band is attributed to complexation and structural perturbation of sorbed tannate by coprecipitated hydroxy Al. The tannate ligands may be adsorbed onto external surfaces and/or incorporated into the structural network of Al precipitates. The FTIR absorption bands observed in Figure 5 are characteristic of the functional groups C=O (1700 or 1725 cm^{-1}), C=C (1598 or 1620, 1501 or 1545 cm^{-1}), O−H (1442 or 1445 cm^{-1}), C−H (1363 or 1330 cm^{-1}) and C−O (1205 or 1220 cm^{-1}) (Sorrell, 1988b). The FTIR absorption bands at 1700 and 1442 cm^{-1} (Figure 5) are indicative of undissociated carboxylic COOH groups and dissociated carboxylate COO$^-$ groups, respectively. The appearance of these bands indicates the presence of partially dissociated tannic acid in the Al precipitates formed in the presence of tannate. Therefore, a portion of the COO$^-$ groups of tannate may be bound to Al during the formation of the Al precipitates under the influence of tannate. The incorporation of tannate into the structure of Al precipitates formed in the presence of tannate was also reported by Violante and Huang (1989) and Colombo *et al.* (2004).

Figure 6 shows the FTIR spectra of the Al precipitates formed at different initial tannate/Al MRs after 40 days of ageing. Compared with the absence of tannic acid (Figure 6a), the Al precipitates formed at a tannate/Al MR of 0.001 had weak absorption bands typical of gibbsite (3615, 3539, 3526, 3465, 3432, 1024,
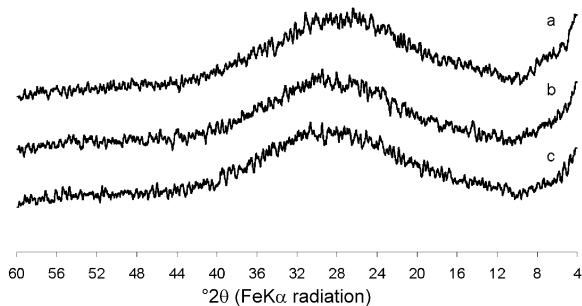

Figure 2. XRD patterns of Al precipitates formed at a tannate/Al molar ratio of 0.1 after ageing for: (a) 1 day; (b) 10 days; and (c) 40 days.
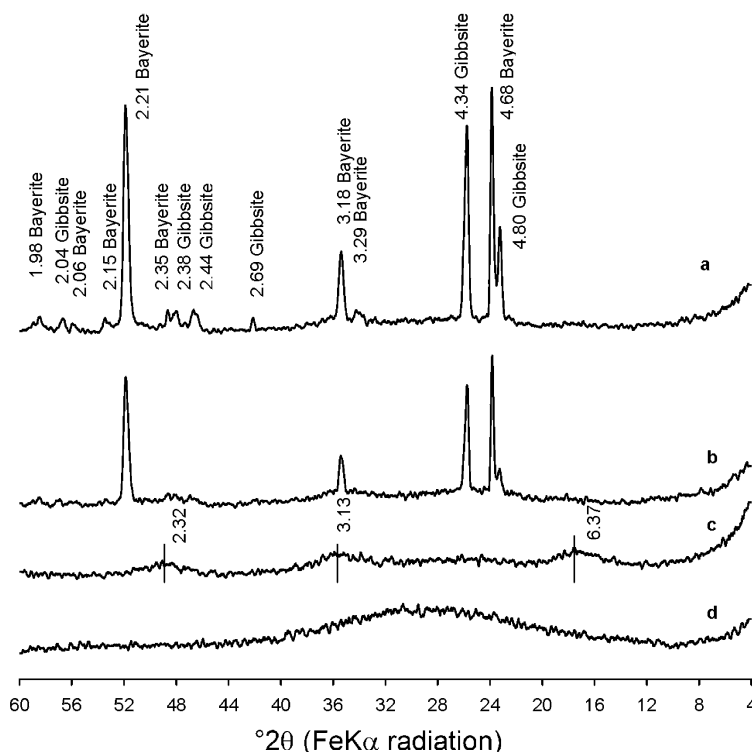
Figure 3. XRD patterns of Al precipitates formed at tannate/Al molar ratios of: (a) 0; (b) 0.001; (c) 0.01; and (d) 0.1 after 40 days of ageing. The *d* values are given in Å. The *d* values of the diffuse peaks at 2.32, 3.13 and 6.37 are characteristic of poorly crystalline boehmite.

970, 559, 532 cm^{-1}) and bayerite (3656 and 769 cm^{-1}) (Figure 6b). When the initial tannate/Al MR was increased to 0.01, most of the absorption bands characteristic of the crystalline Al hydroxides became obscure; the absorption band for gibbsite at 3465 cm^{-1} and that for bayerite at 769 cm^{-1} became much broader (Figure 6c). The impeding effect of tannate is also evident from two additional broad bands at 598 cm^{-1} and 1069 cm^{-1}, which are probably due to −OH

deformation (Farmer, 1975; Krishnamurti and Huang, 1993). Furthermore, a series of new bands (1208−1700 cm^{-1} region) characteristic of tannate were in evidence under this condition.

As the initial tannate/Al MR of 0.01 was increased to 0.1, the characteristic bands of tannate remained intact, but the intensity of these bands was substantially enhanced, and the broad band due to poorly crystalline Al hydroxides virtually disappeared (Figure 6d). One
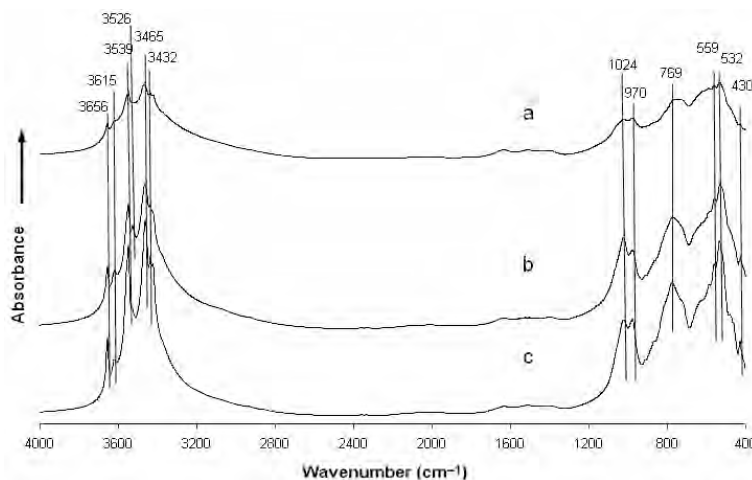

Figure 4. FTIR spectra of Al precipitates formed in the absence of tannate after ageing for: (a) 1 day; (b) 10 days; and (c) 40 days.
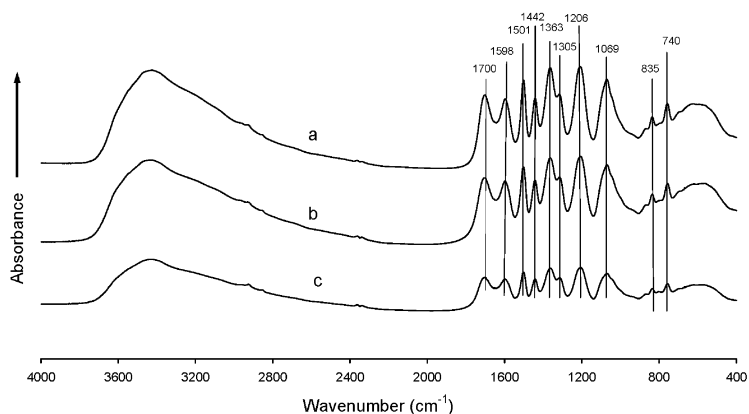
Figure 5. FTIR spectra of Al precipitates formed at a tannate/Al molar ratio of 0.1 after ageing for: (a) 1 day; (b) 10 days; and (c) 40 days.

new band appeared at 740 cm^{-1} (Figure 6d) which is a characteristic band of boehmite (van der Marel and Beutelspacher, 1976). This FTIR evidence (Figure 6d) reinforces the XRD evidence (Figure 3c) and findings of Colombo *et al.* (2004) that indicate that tannate facilitates the formation of boehmite relative to the $Al(OH)_3$ polymorphs when co-precipitated with Al.

^{13}C CPMAS NMR analysis

^{13}C NMR can be used to identify the functional groups bound with carbon, *i.e.* different types of carbon atoms in organic compounds. As shown by the chemical shifts in the ^{13}C NMR spectrum (Figure 7a), tannic acid has functional groups of $-C=O$ (186 ppm), $-COOH$ [163 (and158) ppm], $C=C$ [139 (130 and 112) ppm] and $C-O$ (94 ppm) (Sorrell, 1988a). Compared with pure tannic acid, the ^{13}C CPMAS NMR spectrum of Al precipitates formed at an initial tannate/Al MR of 0.1 basically shows the same major chemical shifts (Figure 7b).

The weak peak at 158 ppm present in the tannic acid in Figure 7a shifted and appeared as a shoulder on the

163 peak in Figure 7b; the 112 ppm peak in Figure 7a increases in intensity in Figure 7b, as do the 139 and 130 ppm peaks. Further, it appears that the 163 ppm peak in Figure 7a splits into three closely positioned peaks in Figure 7b. The changes in those peaks are attributable to complexation of hydroxyl Al with tannate and the resultant structural perturbation of the coprecipitated tannate. A comparison of the ^{13}C NMR spectrum of Al precipitates formed at an initial tannte/Al MR of 0.1 (Figure 7b) and that of tannic acid (Figure 7a) indicates that the Al precipitates formed possessed the same carbon-containing functional groups as tannic acid such as $C=O$, $C=C$, $C-OOH$ and $C-O$, as also demonstrated by the findings of the FTIR study (Figures 5 and 6). Thus, both ^{13}C NMR and FTIR spectroscopies show that tannate was embedded in the Al precipitates.

Adsorbed water, organic carbon and total Al contents

The adsorbed water contents of the freeze-dried Al precipitates formed both in the absence and presence of tannic acid decreased with ageing (Table 1). The
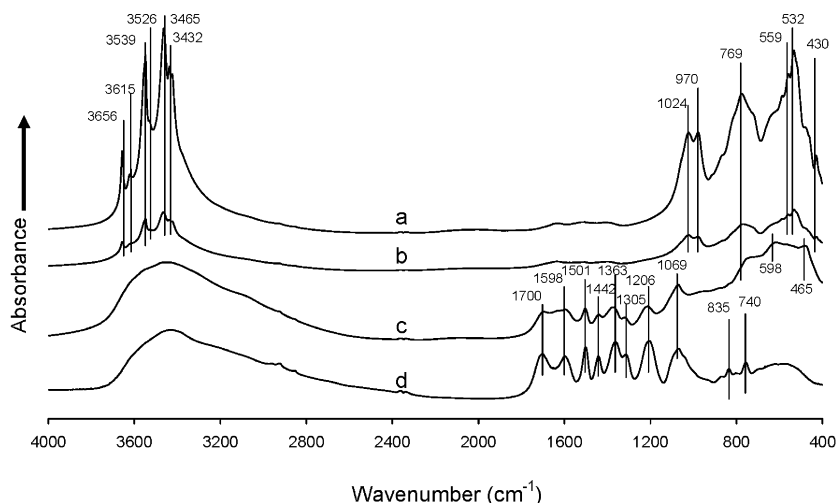

Figure 6. FTIR spectra of Al precipitates formed at tannate/Al molar ratios of: (a) 0; (b) 0.001; (c) 0.01; and (d) 0.1 after 40 days of ageing.
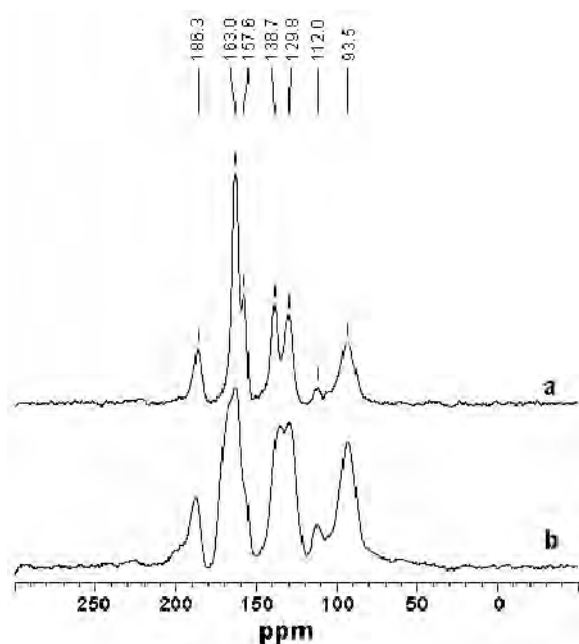
Figure 7. ^{13}C CPMAS NMR spectra of (a) tannic acid and (b) Al precipitates formed at a tannate/Al molar ratio of 0.1 after 40 days of ageing.

adsorbed water contents of the Al precipitates increased with increasing tannate/Al MR. The presence of tannate could enhance the adsorption of water apparently by promoting the penetration of polar water molecules into the poorly crystalline to non-crystalline particles and coordination of the water molecules to the tannate-Al complexes. The increase in the specific surface area of the Al precipitates formed in the presence of tannic acid (discussed below) may also be responsible for some of the increase in the absorbed water.

As the ageing period was extended from 1 to 40 days, the organic C content decreased significantly from 336.6 g/kg to 328.8 g/kg for the Al precipitates formed at an initial tannate/Al MR of 0.1 (Table 1). The organic C content increased with the increasing initial tannate/Al MR (Table 1), indicating that more tannate was incorporated into the structural network of the Al precipitates, through Al complexation by tannate (log K = 3.78) (Kwong and Huang, 1979b and 1981), as the initial tannate/Al MR was increased. This increase in tannate incorporation in the Al precipitates with increasing MR of the initial tannate/Al solution is in accord with the FTIR spectra of Al precipitates formed under the influence of tannic acid, which are essentially dominated by tannate peaks (Figure 6).

The total Al content of the Al precipitates formed at tannate/Al MRs of 0 and 0.1 after 40 days of ageing were 349 and 155 g kg^{-1} (Table 1). The data demonstrate the increased hindering effect of tannate on the precipitation of Al in the solid phase through the process of hydrolytic reactions coupled with increased incorporation of

Table 1. Total Al, organic C and adsorbed water contents and selective dissolution analyses of Al precipitates formed at various initial tannate/Al MR after different ageing periods.

	Initial tannate/Al MR								LSD$_{0.05}$*
	0			0.001	0.01	0.1			
Ageing period (days)	1	10	40	40	40	1	10	40	
Adsorbed water (g/kg)	84±1†	46±5	47±0	85±3	109±1	144±2	139±2	128±1	5
Organic C (g/kg)	0	0	0	9.7±0.7	113.1±0.7	336.6±3.3	334.5±1.4	328.8±1.4	3.2
Total Al (g/kg)	346±21	345±15	349±10	333±10	322±17	148±2	148±10	155±9	31
Pyrophosphate extracted Al (g/kg)	2.5±0.4	2.4±0.4	2.6±1.0	16.0±2.1	32.0±2.9	75.7±1.6	72.0±4.0	62.0±1.4	4.8
Oxalate extracted Al (g/kg)	33.1±0.0	31.6±2.2	30.8±2.7	55.3±1.5	71.3±2.0	78.4±5.9	77.2±1.6	73.3±0.9	6.1

* Least significant difference
† Mean (of duplicate) ± standard error

tannate and water in the precipitates with increasing MR. Ageing did not affect significantly the total Al content of the precipitates (Table 1).

Pyrophosphate-extracted Al

Pyrophosphate-extractable Al content of the Al precipitates formed at the initial tannate/Al MR of 0.1, indicative of organically bound Al, decreased markedly with ageing after 40 days (Table 1). This is in good agreement with the decrease in organic C content with ageing (Table 1).

For the Al precipitates aged for 40 days, pyrophosphate-extracted Al increased substantially as the initial tannate/Al MR increased from 0 to 0.1, indicating that more Al was associated with tannate with increase in the initial tannate/Al MR. This trend is consistent with the FTIR spectra (Figure 6) and organic C contents (Table 1) of these four samples. The absorption bands characteristic of tannate and the organic C contents were enhanced substantially with increase in the initial tannate/Al MR.

Oxalate-extracted Al

Although the XRD patterns of the Al precipitates formed at an initial tannate/Al MR of 0.1 indicate no increase in crystallinity with ageing (Figure 2), the amounts of the oxalate-extractable Al show a trend of a gradual decrease (although not statistically significant) in the content of non-crystalline Al with ageing (Table 1). This finding is consistent with the ageing-induced decrease in the intensity of the FTIR absorption bands characteristic of tannate (Figure 5) and the contents of organic C, pyrophosphate-extractable Al, and adsorbed water (Table 1). The oxalate-extracted Al increased with increasing tannate/Al MR after ageing for 40 days (Table 1). This is consistent with the XRD (Figure 3) and FTIR (Figure 6) data and also provides a quantitative basis for understanding the extent of enhancement of the formation of non-crystalline Al precipitates under the influence of tannate.

Specific surface area and microporosity

The BET specific surface area values of the Al precipitates formed in the absence of tannic acid after 1 and 40 days of ageing were 76 and 19 m^2/g (Table 2); whereas those determined by the EGME method were 169 and 132 m^2/g (Table 2). The results obtained from the BET and EGME methods had the same trend in terms of specific surface area. However, the values measured by the EGME retention method were substantially greater than those by the N_2-BET method. The difference could be attributed to a few reasons. The N_2-BET method requires that the sample must be degassed to remove adsorbed molecules under a high vacuum (5−10 mTorr) and this procedure may result in the collapse of precipitates and alter the surface area (Yates, 1975). On the other hand, the calculation of

surface area by the EGME method is based on the assumption that EGME forms a monomolecular layer and that the unit weight of the EGME molecule has a constant surface area (Carter *et al.*, 1986; Tiller and Smith, 1990). However, EGME surface area may not be constant as the molecule may change with the nature and shape of the minerals (Lowell and Shields, 1991). Further, EGME is a dipole molecule. The specific surface area determined by the EGME retention method involves dipole interactions of EGME with the surface or H-bonding formation. Multimolecular layers rather than the assumed monomolecular layer of EGME may be formed particularly on rough surfaces and on porous materials (Cornell and Schwertmann, 1996). This may result in an overestimate of the specific surface area of a sample. However, the data from both BET and EGME methods show that the specific surface area of the Al precipitates formed at the initial tannate/Al MR of 0 decreased with ageing (Table 2), supporting the conclusion that the degree of crystallinity of Al precipitates increases with ageing (Figure 1).

The BET specific surface area values of the Al precipitates formed at an initial tannate/Al MR of 0.1 after 1 and 40 days of ageing were 214 and 186 m^2/g, respectively (Table 2); the respective EGME specific surface area values were much greater when compared with the BET values in this case as well (Table 2). The data obtained by both BET and EGME methods show that the specific surface area of the precipitates increased with increasing the initial tannate/Al MR. This is attributed to structural perturbation of the Al precipitates by tannate ligands through complexation with Al and subsequent exposure of irregular surfaces. The effect of tannate on increasing both BET and EGME specific surface area values of the Al precipitates of our study supports the trend of the EGME specific surface areas of the Al precipitates reported by Kwong and Huang (1981). Furthermore, our data show that tannate ligands complexed with structural Al stabilized the

Table 2. The specific surface area of Al precipitates formed under the influence of tannate and ageing.

Tannate/Al MR	Ageing period (days)	Specific surface area (m^2/g)	
		EGME	BET
0	1	169±18*	75.6±1.0
0	10	167±21	n.d.
0	40	132±18	19.2±0.3
0.001	40	350±42	109.2±0.5
0.01	40	488±21	114.6±0.5
0.1	1	599±21	213.5±0.1
0.1	10	581±12	n.d.
0.1	40	557±16	185.8±0.9
$LSD_{0.05}$[†]		53	1.5

* Mean (of duplicate) ± standard error
[†] Least significant difference
n.d. not determined

Table 3. Average pore diameter and microporosity of Al precipitates formed at various initial tannate/Al MR after 40 days of ageing.

Minerals	Tannate/Al MR				$LSD_{0.05}$*
	0 Bayerite and gibbsite	0.001 Poorly crystalline	0.01 Non-crystalline	0.1 Non-crystalline	
Micropore area (m^2 g^{-1})	0	12.0±0.5[†]	14.9±0.1	43.8±0.8	1.4
Average pore diameter (nm)	6.6±0.3	5.0±0.0	3.5±0.1	2.4±.0.1	0.5

[†] Mean (of duplicate) ± standard error
* Least significant difference

amorphous network (Figure 2) and maintained a high specific surface area upon ageing (Table 2).

The BET analyses show for the first time the effect of tannate on the porosity of Al precipitates (Table 3). Micropores are developed as a result of crystal defects and the formation of small particle size. The stack of the materials with small size particles may form micropores among particles if the particle size is small enough. The presence of tannate during the formation of Al hydroxides triggered the formation of microporosity, decreased the average pore size and enhanced the micropore specific surface area (Table 3) through structural perturbation (Figures 2 and 6).

PZSE

Charge develops on the hydroxylated surface of Al precipitates either through amphoteric proton association to and dissociation from the surface hydroxyl groups (Parks, 1967; Van Raij and Peech, 1972; Gast, 1977). The PZSE values of the Al precipitates formed at any particular initial tannate/Al MR (Table 4) show a slight but not statistically significant decrease after 40 days of ageing as compared to 1 day of ageing.

The PZSE of the Al precipitates formed under the influence of tannate substantially decreased with the

increase of the initial tannate/Al MR both after 1 and 40 days of ageing (Table 4). This is attributed to the increase in the removal of the surface-bound H_2O by tannate co-precipitation, and/or tannate adsorption on the Al precipitates, resulting in the enhancement of the exposure of COO^- groups of tannate and the increase in the development of negative charge on their surfaces. This interpretation is substantiated by the observation that the C content of Al precipitates (Table 1) and the intensity of the FTIR absorption band at 1442 cm^{-1} (characteristics of COO^- in the FTIR spectra) (Figure 6) as well as pyrophosphate-extracted Al contents (Table 1) increased consistently with the increase of the initial tannate/Al MR.

CONCLUSIONS AND ENVIRONMENTAL SIGNIFICANCE

The role of organic substances in influencing Al transformation in the environment is well documented (Kwong and Huang, 1975, 1981; Lind and Hem, 1975; Kodama and Schnitzer, 1980; Huang and Violante, 1986; Sposito, 1996; Huang *et al.*, 2002; Colombo *et al.*, 2004). However, the combined effects of organics and ageing on the structural configuration in relation to the surface and charge properties of the Al precipitates formed remains obscure. The data obtained in the present study reveal for the first time, the fact that structural perturbation of Al precipitates through co-precipitation of tannate with Al and adsorption of tannate on the surface of the poorly crystalline to non-crystalline structural network, resulted in a decrease in the average pore size and the development of microporosity with an enhancement of the specific surface area and a decrease of the PZSE.

Ageing of Al precipitates formed in the absence of tannate resulted in a decrease in their specific surface area due to their increased crystallinity. In contrast, ageing had much less of an effect on the specific surface area of Al precipitates formed at a tannate/Al MR of 0.1. Tannate stabilized the short-range ordered structural network and thus maintained a large specific surface area during ageing. There was no discernable change in the XRD data of the Al precipitates formed under the

Table 4. PZSE values of Al precipitates formed at different tannate/Al MR after 1 day and 40 days of ageing.

Tannate/Al MR	Ageing period (days)	PZSE
0	1	10.3±0.4*
	40	9.9±0.8
0.001	1	9.2±0.4
	40	8.8±0.3
0.01	1	7.4±0.2
	40	7.2±0.7
0.1	1	5.0±0.1
	40	4.8±0.4
$LSD_{0.05}$[†]		1.1

* Mean (of duplicate) ± standard error
[†] Least significant difference

influence of tannate upon ageing. However, the organic C contents, the pyrophosphate- and oxalate-extractable Al, and adsorbed water contents decreased with ageing, indicating an increase in the degree of ordering of the Al precipitates formed. Despite this, any significant change in the PZSE of Al precipitates formed both in the absence and presence of tannate was not observed due to ageing.

As micropores can adsorb organic molecules which are not accessible to microorganisms and enzymes due to steric hindrance, the microporous structure of environmental particles play a very important role in the stabilization of natural organics and xenobiotics (de Jong, 2000; Haider and Guggenberger, 2005). Therefore, the role of organic substances in the structural perturbation and in the development of microporosity of Al transformation products and the impact on their surface and charge properties caused by tannic acid in the present study merit close attention to help us understand better the dynamics, mechanisms and fate of nutrients and pollutants in soil and associated environments.

REFERENCES

Berry, L.G. (1974) *Selected Powder Diffraction Data for Minerals*. Joint Committee on Powder Diffraction Standards, 1601 Park Lane, Swarthmore, PA.

Bertsch, P.M. and Bloom, P.R. (1996) Aluminum. Pp. 517–550 in: *Methods of Soil Analysis. Part 3. Chemical Methods*. SSSA Book Series no. 5. (D.L. Sparks, editor). Soil Science Society of America and American Society of Agronomy, Madison, Wisconsin.

Carter, D.L., Mortland, M.M. and Kemper, W.D. (1986) Specific surface. Pp. 413–423 in: *Methods of Soil Analysis: Part 1. Physical and Mineralogical Methods*, 2nd edition (A. Klute, editor). Agronomy Monograph no.9. Soil Science Society of America and American Society of Agronomy, Madison, Wisconsin.

Colombo, C., Ricciardella, M., Cerce, A.D., Maiuro, L. and Violante, A. (2004) Effects of tannate, pH, sample preparation, ageing and temperature on the formation and nature of Al oxyhydroxides. *Clays and Clay Minerals*, **52**, 721–733.

Cornell, R.M. and Schwertmann, U. (1996) *The Iron Oxides. Structure, Properties, Reactions, Occurrence and Uses*. VCH, Weinheim, Germany.

Daintith, J. (1990) *A Concise Dictionary of Chemistry*. New Edition. Oxford University Press, Oxford, UK.

de Boer, J.H., Lippens, B.C., Linsesn, B.G., Broeckhoff, J.P., Heuval, A. and Osinga, T.J. (1966). The *t*-curve of multi-layer N_2-adsorption. *Journal of Colloid and Interface Science*, **21**, 405–414.

de Jong, H. (2000) The microporous structure of organic and mineral soil materials. *Soil Science*, **165**, 99–108.

Eltantawy, I.M. and Arnold, P.W. (1973) Reappraisal of ethylene glycol monoethyl ether (EGME) method for surface area estimation of clays. *Journal of Soil Science*, **24**, 232–239.

Farmer, V.C. (1975) Infrared spectroscopy in mineral chemistry. Pp. 357–388 in: *Physicochemical Methods of Mineral Analysis* (A.W. Nicol, editor). Plenum Press, New York.

Gardner, W.H. (1986) Water content. Pp. 493–544 in: *Methods of Soil Analysis, Part 1. Physical and Mineralogical Methods*, 2nd edition (A. Klute, editor). Agronomy Monograph no. 9. Soil Science Society of America and American Society of Agronomy, Madison, Wisconsin.

Gast, R.G. (1977) Surface and colloid chemistry. Pp. 27–73 in: *Minerals in Soil Environments*. (J. B. Dixon and S.B. Weed, editors). Soil Science Society of America, Madison, Wisconsin.

Goh, T.B., Violante, A. and Huang, P.M. (1986) Influence of tannic acid on retention of copper and zinc by aluminum precipitation products. *Soil Science Society of America Journal*, **50**, 820–825.

Gregg S.L. and Sing K.S.W. (1982) *Adsorption Surface Area and Porosity*, 2nd edition. Academic Press, London, UK.

Haider, K. and Guggenberger, G. (2005) Soil minerals and organic components: impact on biological processes, human welfare and nutrition. Pp. 3–16 in: *Soil Abiotic and Biotic Interactions and Impact on the Ecosystem and Human Welfare*. (P.M. Huang, A. Violante, J.-M. Bollag and P. Vityakon, editors). Science Publisher, Enfield, New Hampshire.

Hsu, P.H. (1989) Aluminum hydroxides and oxyhydroxides. Pp. 331–378 in: *Minerals in Soil Environments*, 2nd edition (J.B. Dixon and S.B. Weed, editors). SSSA Book Series, no. 1. Soil Science Society of America, Madison, Wisconsin.

Huang, P.M. (1988) Ionic factors affecting aluminum transformations and the impact on soil and environmental science. *Advances in Soil Science*, **8**, 1–78.

Huang, P.M. (1995). The role of short range ordered mineral colloids in abiotic transformation of organic components in the environment. Pp. 135–167 in: *Environmental Impact of Soil Component Interactions* (P.M. Huang, J. Berthelin, J.-M. Bollag, W.B. McGill and A.L. Page, editors). Lewis Publishers, Boca Raton, Florida.

Huang, P.M. and Violante, A. (1986) Influence of organic acids on crystallization and surface properties of precipitation products of aluminum. Pp. 159–221 in: *Interactions of Soil Minerals with Natural Organics and Microbes* (P.M. Huang and M. Schnitzer, editors). SSSA Special Publication 17. Soil Science Society of America, Madison, Wisconsin.

Huang, P.M., Wang, M.K., Kampe, N. and Schulze, D.G. (2002) Aluminum hydroxides. Pp. 261–289 in: *Soil Mineralogy with Environmental Applications*. SSSA Book Series, no.7. Soil Science Society of America, Madison, Wisconsin.

Kodama, H. and Schnitzer, M. (1980) Effect of fulvic acid on the crystallization of aluminum hydroxides. *Geoderma*, **24**, 195–205.

Krishnamurti, G.S.R. and Huang, P.M. (1993) Formation of lepidocrite from iron (II) solutions: stabilization by citrate. *Soil Science Society of America Journal*, **57**, 861–867.

Kwong, Ng Kee K.F. and Huang, P.M. (1975) Influence of citric acid on the crystallization of Al precipitation products. *Clays and Clay Minerals*, **23**, 164–165.

Kwong, Ng Kee K.F. and Huang, P.M. (1977) Influence of citric acid on the hydrolytic reactions of aluminum. *Soil Science Society of America Journal*, **41**, 692–697.

Kwong, Ng Kee K.F. and Huang, P.M. (1978) Nature of hydrolytic precipitation products of aluminum as influenced by low-molecular-weight complexing organic acids. Pp. 527–536 in: *Proceedings of the VI International Clay Conference, Oxford* (M.M. Mortland and V.C. Farmer, editors). Elsevier, Amsterdam, the Netherlands.

Kwong, Ng Kee K.F. and Huang, P.M. (1979a) Surface reactivity of aluminum hydroxides precipitated in the presence of low molecular weight organic acids. *Soil*

Science Society of America Journal **43**, 1107−1113.

Kwong, Ng Kee K.F. and Huang, P.M. (1979b) The relative influence of low-molecular-weight, complexing organic acids on the hydrolysis and precipitation of aluminum. *Soil Science*, **128**, 337−342.

Kwong, Ng Kee K.F. and Huang, P.M. (1981) Comparison of the influence of tannic acid and selected low-molecular-weight organic acids on precipitation products of aluminum. *Geoderma*, **26**, 179−183.

Lim, C.H.L. and Jackson, M.L. (1982) Dissolution for total elemental analysis. Pp. 1−12 in: *Methods of Soil Analysis, Part 2. Chemical and Mirobiological Properties*. Agronomy monograph No. 9 (A.L. Page, R.H. Miller and D.R. Keeney, editors). Soil Science Society of America and American Society of Agronomy, Madison, Wisconsin.

Lind, C.J. and Hem, J.D. (1975) *Effects of Organic Solutes on Chemical Reactions of Aluminum.* US Geological Survey, Water Supply Paper 1827-G.

Lowell, S. and Shields, J.E. (1991) *Powder Surface Area and Porosity*, 3rd edition. Chapman and Hall, New York.

McKeague, J.A. and Day, J.H. (1966) Dithionite- and oxalate-extractable Fe and Al as aids in differentiating classes of soils. *Canadian Journal of Soil Science*, **46**, 13−22.

Parks, G.A. (1967) Aqueous surface chemistry of oxides and complex oxide minerals. Isoelectric point and zero point of charge. Pp. 121−160 in: *Equilibrium Concepts in Natural Water Systems.* (R.F. Gould, editor). Advances in Chemistry Series **67**. American Chemical Society, Washington, D.C.

Ravikovitch, P.I. and Neimark, A.V. (2000) Calculations of pore size distribution in nanoporous materials from adsorption desorption isotherms. *Studies in Surface Science and Catalysis*, **129**, 597−606.

Sakurai, K., Ohadate, Y. and Kyuma, K. (1988) Comparison of salt titration and potentiometric titration methods for the determination of zero point of charge (ZPC). *Soil Science and Plant Nutrition*, **34**, 171−182.

Sakurai, K., Ohdate, Y. and Kyuma, K. (1989) Potentiometric automatic titration (PAT) method to evaluate zero point of charge (ZPC) of variable charge soils. *Soil Science and Plant Nutrition*, **35**, 89−100.

Singer, A. and Huang, P.M. (1990) The effect of humic acid on the crystallization of precipitation products of aluminum. *Clays and Clay Minerals*, **38**, 47−52.

Sorrell, N.T. (1988a) Chapter 4. ^{13}C Nuclear Magnetic Resonance. Pp. 97−115 in*: Interpreting Spectra of Organic Molecules* (N.T. Sorrel, editor). University Science Books, Mill Valley, California.

Sorrell, N.T. (1988b) Chapter 2. Infrared spectroscopy. Pp. 11−52 in*: Interpreting Spectra of Organic Molecules* (N.T. Sorrel, editor). University Science Books, Mill Valley, California.

Sposito, G. (1996) *The Environmental Chemistry of Aluminum,* 2nd edition. CRC Press, London, 464 pp.

Stevenson, F.J. (1994) *Humus Chemistry. Genesis, Composition, Reactions.* 2nd edition. John Wiley & Sons, New York.

Storck, S., Bretinger, H. and Maier, W.F. (1998) Characterization of micro- and mesoporous solids by physisorption methods and pore-size analysis. *Applied Catalysis A: General*, **174**, 137−146.

Tiller, K.G. and Smith, L.H. (1990) Limitations of EGME retention to estimate the surface area of soils. *Australian Journal of Soil Research*, **28**, 1−26.

van der Marel, H.W. and Beutelspacher, H. (1976) Aluminum minerals. Pp. 194−195 in: *Atlas of Infrared Spectroscopy of Clay Minerals and their Admixtures* (H.W. van der Marel and H. Beutelspacher, editors). Elsevier, Amsterdam.

Van Raij, B. and Peech, M. (1972) Electrochemical properties of some Oxisols and Alfisols of the Tropics. *Soil Science Society of America Journal*, **36**, 587−593.

Violante, A. and Huang, P.M. (1984) Characteristics and surface properties of pseudoboehmites formed in the presence of selected organic and inorganic ligands. *Soil Science Society of America Journal*, **48**, 1193−1201.

Violante, A. and Huang, P.M. (1985) Influence of inorganic and organic ligands on the formation of aluminum hydroxides and oxyhydroxides. *Clays and Clay Minerals*, **33**, 181−192.

Violante, A. and Huang, P.M. (1989) Influence of oxidation treatments on surface properties and reactivities of short-range ordered precipitation products of aluminum. *Soil Science Society of America Journal*, **53**, 1402−1407.

Violante, A. and Violante, P. (1980) Influence of pH, concentration and chelating power of organic anions on the synthesis of aluminum hydroxides and oxyhydroxides. *Clays and Clay Minerals*, **28**, 425−434.

Wang, D. and Anderson, D.W. (1998) Direct measurement of organic carbon in soils by the Leco 12 Carbon Analyzer. *Communications in Soil Science and Plant Analysis*, **29**, 15−21.

Yates, D.E. (1975) The Structure of the Oxide/aqueous Electrolyte Interface. PhD thesis, University of Melbourne, Australia.